Design and Performance Evaluation of an Axial Flux PM Generator for Micro-Wind Applications

E. ORTIZ-GARCIA[1], JUAN M. RAMIREZ[1], JOSÉ RAFAEL DORREGO-PORTELA[2]

[1]Department of Electrical Engineering
Center for Research and Advanced Studies, Center for Research and Advanced Studies, Zapopan, 45019, Jalisco, MEXICO

[2]Division of Graduate Studies
Universidad del Istmo, Universidad del Istmo, Santo Domingo Tehuantepec, 70760, Oaxaca, MEXICO

Corresponding author: joramirez@cinvestav.mx

Abstract: - This research introduces a novel 1 kW axial-flux permanent magnet synchronous generator (AF-PMSG) designed specifically for low-power wind turbines. Employing magnetic circuit theory, we developed a systematic design process and conducted rigorous performance analyses under various operating conditions. MATLAB simulations were validated through 3D Finite Element Analysis and experimental testing, ensuring the accuracy of our model. The generator achieved a maximum efficiency of 87.7% and maintained consistent performance across a wide range of wind speeds. Compared to traditional generators, the axial-flux topology significantly increases power density, making it an ideal choice for small-scale wind energy applications.

Key-Words: - Electric machine design, Energy conversion, Finite element analysis, Permanent magnet machines, Wind energy

Received: March 12, 2024. Revised: August 6, 2024. Accepted: September 15, 2024. Published: October 29, 2024.

1 Introduction

Considering the transition towards using renewable energy sources, the research and development of low-power turbines becomes relevant. It is necessary to propose efficient and economical solutions for their use in microgrids, remote areas and decentralised projects. Thus, this work proposes the design of a low-power turbine that maximises efficiency and reduces costs [1]-[2]. Historically, the global strategy in the wind sector has favoured the development of large-capacity turbines.

This trend has dominated the market with large companies, which limits innovation and creates a dependency on introducing new technologies due to confidentiality issues [1]-[3]. Low-power turbines (SWTs) represent an excellent potential for future sustainable development. Unlike their high-power counterparts, SWTs are suitable for homes, farms, and rooftops. Their success rests on the intelligent design to capture energy efficiently even in moderate winds, making them ideal for locations with lower wind patterns, minimising noise and maintenance needs, which is a more comfortable solution. By prioritising efficiency, noise reduction and low cost, SWT designs bring clean, renewable energy to many users, leading to sustainable development.

In this paper, a low-power turbine with a permanent magnet synchronous generator is employed due to the need to overcome the limitations and maximise energy conversion efficiency. These generators represent a viable and appropriate design option, minimising energy losses and optimising the conversion of wind into electricity [4]-[6].

In [7], a 1 kW generator is connected to an AG700 wind turbine, and the electrical grid is used; it consists of a stator placed between 2 rotors with permanent magnets. During the tests, the electrical parameters were verified and compared with simulations. At a nominal speed of 400 rpm, the

generator produces a voltage of 75 V with a THD of 7.1 and achieves an efficiency of 73%.

Reference [8] outlines a design for an axial flux permanent magnet synchronous generator suitable for wind power. This design takes into account the varying widths of the magnets and coils relative to the generator's radius. The analytical model is confirmed through experiments, proving its value in optimising the generator's structure and operation.

This research aims to develop a highly efficient wind energy conversion system utilising a permanent magnet synchronous generator. Key objectives include:

Technology review: Surveying existing wind turbine technologies and magnet configurations, focusing on low-frequency turbines [9]-[10].

Generator and rotor design: Designing a generator and rotor that maximises power output and efficiency [11].

Performance evaluation: Conducting simulations and physical prototyping to assess system performance.

Advantages of Permanent Magnet Synchronous Generators:

Simplified design: Reduced energy losses and increased efficiency due to a more straightforward design.

Enhanced reliability: Eliminating brushes and slip rings leads to higher reliability and lower maintenance costs.

Optimised operational costs: Minimised maintenance and long-term operational costs.

Focus on Low-Power Turbines:

Advantages: Higher power density, reduced maintenance, and accessibility due to affordable materials and local manufacturing.

Addressing energy access: Democratising energy access in regions with limited infrastructure.

Decentralised solutions: Promoting energy system resilience and diversification.

Sustainable energy future: Optimising efficiency, reducing costs, and addressing challenges of small-scale power generation.

Key Contribution:

This research contributes to the field of electrical machines by optimising the design of permanent magnet synchronous generators for wind energy conversion, focusing on low-power applications. This optimisation is crucial for efficient energy conversion and sustainable energy solutions.

Energy savings: the authors use an efficient design that minimises electrical losses during the energy conversion process, resulting in lower costs and reduced environmental impact.

Optimal performance: careful design to ensure that the machine is correctly matched to the application, considering factors such as motor speed, output torque, and generator efficiency, as well as robust design to minimise maintenance requirements. Safety and function: the device must operate safely and effectively within its environment, considering heat dissipation, electromagnetic interference, and compatibility with other systems.

Thus, this paper presents an efficient, careful, and functional design vital for electrical machines to perform their functions effectively, saving energy, ensuring reliability, and operating safely. In this research, a permanent magnet synchronous generator and wind turbine have been designed and constructed to meet the most demanding standards.

2 Prototyping design

This section describes the design process, from selecting the critical parameters to implementing the design methodology. The proper selection of the parameters is essential for the optimal performance of the permanent magnet synchronous machine. One of the crucial aspects is the magnetic flux density (B_{max}), which is determined by specific operational requirements, such as power output and mechanical torque. Through iterative calculations and simulations, the value of B_{max} is set to ensure efficient magnetic flux distribution and to avoid saturation in the circuit. The fundamental magnetic configuration of the synchronous machine with a dual gap is depicted in Fig. 1. The structure is assumed to be replicated indefinitely in both directions. In a rotating system generating torque, the ends would be situated at the machine's centre, resulting in a limited number of magnetic poles. It can be observed that the rotor is composed of magnets with alternating polarities, separated by nonmagnetic spacers, which could be made of air and attached to a ferromagnetic iron core.

On the other hand, the stator comprises windings encapsulated in resin.

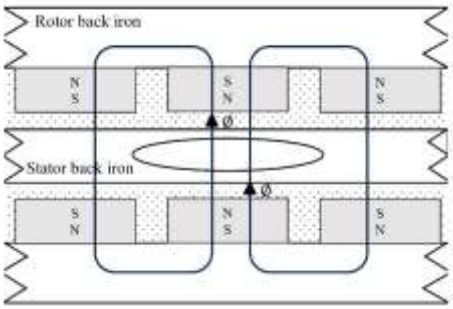

Fig. 1. Basic magnetic structure of the PMSG.

The magnetic circuit consists of a magnetomotive force (MMF) produced by the magnets and a series of reluctances. The MMF is analogous to the voltage in a standard electrical circuit, reluctance is analogous to resistance, and magnetic flux is analogous to current. In addition to the air gap reluctance, there is also reluctance associated with the magnets and the rotor to which they are attached. Once all generator components have been considered, they can be modelled as a magnetic circuit, Fig. 2.

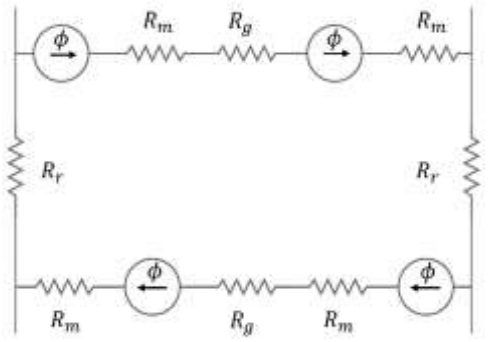

Fig. 2. Magnetic circuit model.

The design process of the PMSG involves several key steps. It starts with defining specific requirements, including the output power and operating conditions. The frequency and machine revolutions ratio determines the number of magnetic poles (N_m) in the rotor design and is denoted by the following expression.

$$N_m=\frac{120\,f_e}{s_r} \tag{1}$$

where f_e is the electrical frequency in Hz, and s_r the rated speed in rpm.

The primary constraint of (1) is that N_m must be an even integer. If N_m is an odd number or a fraction, N_m must be modified to produce an even integer. After this, S_r is recalculated according to (1). Given two poles form permanent magnets, the pole pairs are obtained from the following expression

$$N_p=\frac{N_m}{2} \tag{2}$$

where N_p is the number of pole pairs.

Minimising the weight and volume of the magnet is an essential factor in achieving an efficient design. In this regard, maximum energy BH_{max} is crucial for choosing and sizing the magnets. The minimum volume of the PMSG magnet can be found as follows,

$$V_m=\frac{T_m}{BH_{\max}N_m} \tag{3}$$

The mechanical torque of the machine is given by.

$$T_m=\frac{P_{\text{int}}}{\omega_m} \tag{4}$$

where T_m is the input mechanical torque, P_{int} is the input mechanical power coming from the wind turbine, and ω_{m} is the input mechanical speed in rad/s. These parameters are given by.

$$P_{\text{int}}=\frac{P_{out}}{\eta} \tag{5}$$

$$\omega_m=\frac{2\pi s_r}{60}=\frac{2\pi f_e}{N_p} \tag{6}$$

where η is the efficiency for the generator design according to the NEMA MG 1-2009 and IEC 60034-30-1 standards; the efficiency for this power is $\eta >$ 85%. The mechanical speed (ω_{m}) is also related to the electrical frequency (f_e) and the number of pole pairs (N_p).

The next step is to calculate the thickness length of the magnet (l_m) in terms of the face area of the air gap magnet and the stator through the axial length of the generator (L), finding the parameters for the V_m calculation,

$$l_m=\frac{V_m}{A_m} \tag{7}$$

$$A_m=\frac{\tau_m}{\tau_p} \tag{8}$$

The magnetic pole steps on the internal and external radii are obtained with the expressions below,

$$\tau_{pi}=R_{si}\theta_p \tag{9}$$

$$\tau_{pi}=R_{so}\theta_p \quad (10)$$

where $\boldsymbol{\theta}_p$ is the polar angular step. The subscripts "*si*" and "*so*" denote the internal and external radii, respectively, as shown in Fig. 3.

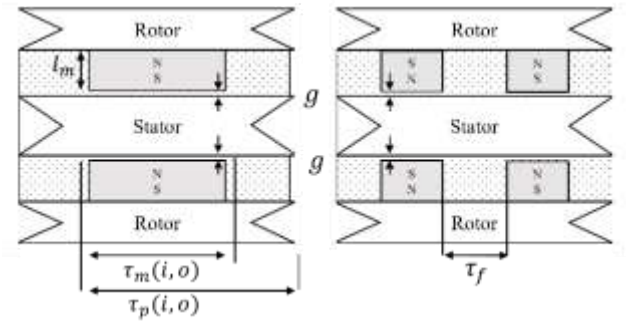

Fig. 3. Magnet geometry

The optimal size of the magnet is typically verified by

$$MAR=\frac{l_m}{\alpha_m\tau_p}\leq 0.25 \quad (11)$$

The relationship $4\leq\frac{l_m}{g}\leq 5$ and the magnetic fraction α_m

The efficiency of the PMSG is given by

$$\eta=\frac{P_{out}}{P_{\text{int}}}100=\frac{T\omega_m-P_c-P_{mis}-P_{nuc}}{T\omega_m}100 \quad (12)$$

$$P_c=N_{ph}I_{ph}^2R_{ph} \quad (13)$$

$$P_{nuc}=\rho_{bi}V_{st}\Gamma(B_{\max}F_e) \quad (14)$$

$$P_{mis}=0.01P_{\text{int}}=0.001T\omega_m \quad (15)$$

where P_c represents copper losses, P_{nuc} represents core losses, and P_{mis} represents miscellaneous losses. This iterative process is observed in the algorithm used in the design and is illustrated in Fig. 4.

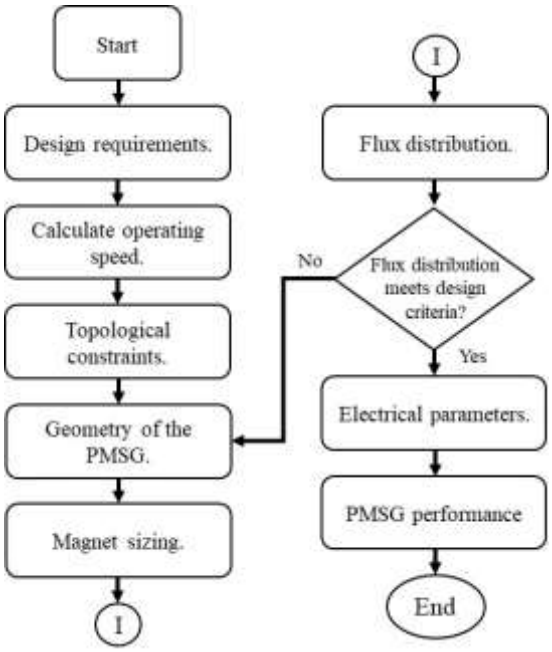

Fig. 4. PMSG design flowchart.

3 Performance Analysis

This section comprehensively analyses the generator's performance across various operations applied to a low-power wind turbine. The design methodology, illustrated in Figure 4, allows for determining the generator's geometry, as shown in Table 1 and Figure 5.

For this analysis, a detailed comparison was made between the results obtained through finite element method (FEM) simulations and the experimental data collected during prototype testing. The experimental tests were conducted in a controlled environment, which minimised the influence of external factors and ensured the repeatability of the results. The analysis includes both the electrical performance of the generator and its mechanical behaviour under various operating conditions.

Table 1: Geometry definitions

Geometry	Value	Unit	Geometry	Value	Unit
R_{so}	190	mm	R_{so}	55.4	mm
R_{si}	79.0	mm	R_{so}	25.4	mm
R_{ro}	150	mm	R_{so}	18.0	mm
R_{ri}	29.5	mm	R_{so}	38.0	mm
τ_f	30.0	mm	R_{so}	72.0	mm
τ_m	50.8	mm	R_{so}	14.7	mm
τ_{po}	55.4	mm	R_{so}	92.0	mm

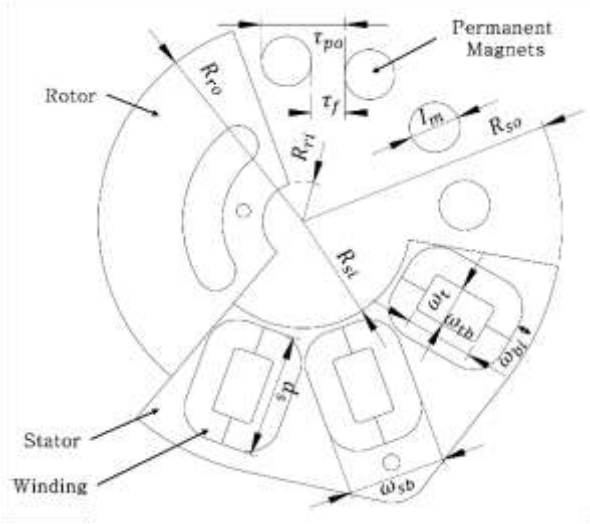

Fig. 5. Geometric Parameters.

3.1 Prototype Design

The construction of the generator prototype begins with the cutting and stacking of silicon steel sheets to form the rotor, improving its magnetic performance and reducing losses, as shown in Figure 6. Neodymium magnets are mounted on the rotor, while the copper coils for the stator are precisely manufactured, ensuring exact placement and proper insulation to minimise potential electrical issues. These coils are encapsulated in epoxy resin to increase their durability, as seen in Figure 7. Finally, the generator is assembled along with the wind turbine rotor, and the design is verified through simulations and experimental testing to ensure it meets the specifications.

The turbine prototype was implemented, as shown in Figure 8, and consists of the following components: 1) the rotor hub, which connects the blades to the generator and transmits wind force; 2) the blades, aerodynamically designed to capture wind energy; 3) the shaft, which functions as the transmitter of energy from the rotor to the generator; 4) the permanent magnet synchronous generator (PMSG), which converts mechanical energy into electrical energy; and 5) the tail vane, which aligns the turbine in the direction of the wind to maximise energy capture efficiency.

Fig. 6. Stacking of rotor laminations.

Fig. 7. Coils' manufacturing and encapsulation.

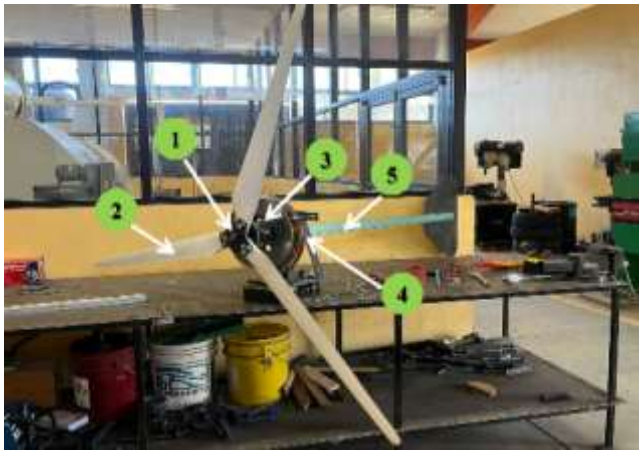

Fig. 8. Prototype of the wind turbine based on the PMSG

3.2 Magnetic Flux

Figure 9 shows the magnetic flux distribution of the PMSG, highlighting the magnetic flux density at nominal speed. The results indicate that these fluctuations remain within safe operational limits, ensuring no magnetic saturation or overheating of the components. This behaviour is crucial to maintaining high generator performance, as it ensures proper interaction between the rotor and stator throughout the entire operating range.

The variations in magnetic flux density, presented in Figure 10, show the different maximum and minimum flux points as the rotor rotates, highlighting three fundamental values: a) B_{max} (T): Represents the maximum density. Throughout the RPM range (from 50 to 550), the flux remains constant at around 1.7 T, indicating that the generator operates efficiently without reaching magnetic saturation levels, even at

higher speeds; b) B_{pro} (T): Reflects the average density, which remains constant around 1 T across all RPMs. This suggests good magnetic stability in the generator, and c) B_{min} (T): The minimum density remains close to 0 T throughout the RPM range. This value indicates that although the flux varies over time and during the generator's rotation cycle, it does not fall below 0 at any significant point, suggesting a low likelihood of magnetic flux losses.

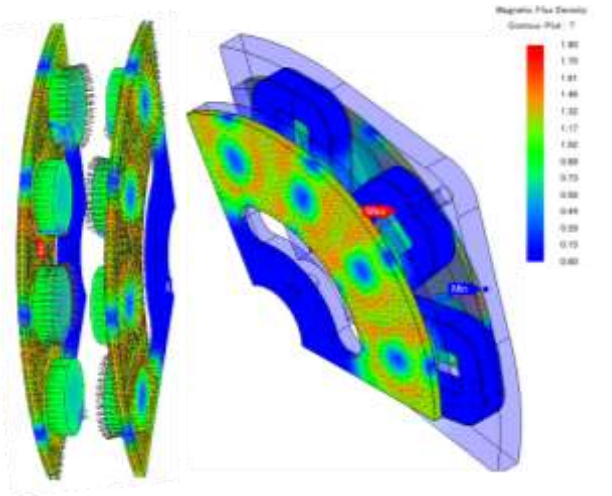

Fig. 9. Rotor's magnetic flux.

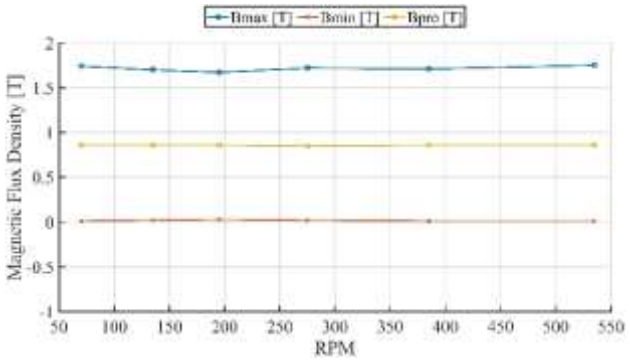

Fig. 10. magnetic flux at the terminals of the PMSG.

3.3 Voltage

As part of this analysis, voltage measurements were taken at the generator terminals over various operations. Fig. 11 illustrates how the PMSG voltage varies as a function of speed and applied load, providing a fundamental understanding of the relationship between rotor speed and generated voltage. It is essential to observe this proportionality and evaluate how different load conditions affect the voltage, as under 100% load, the voltage decreases due to the internal voltage drop of the generator. This figure shows that the PMSG reaches a voltage of 115 V at nominal speed without load and a voltage of 105 V at nominal speed with a 100% load.

Additionally, Fig. 12 illustrates the percentage difference in the results, allowing for a detailed assessment of voltage variation under different load and speed conditions. This information is crucial for understanding the efficiency and stability of the PMSG in practical applications.

Figure 13 visually compares voltage signals from the wind turbine prototype, contrasting simulated and measured voltages over time. For a speed of 135 rpm, the simulation shows a voltage of 43.37 V, while the measurement records 38.46 V, resulting in an 11.32% deviation. At 275 rpm, the simulation yields 92.95 V compared to 89.27 V from the measurements, indicating a 3.94% variation. Although both data sets exhibit similar trends, significant differences are observed in voltage peaks and magnitudes. Despite these discrepancies, the overall behaviour of the voltage signals remains consistent, suggesting a general agreement between the simulated and measured results.

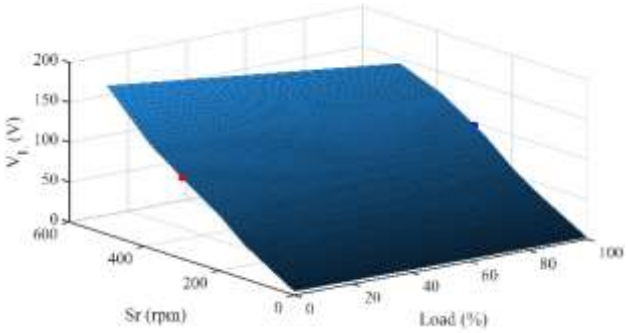

Fig. 11. Voltage as a function of speed and load.

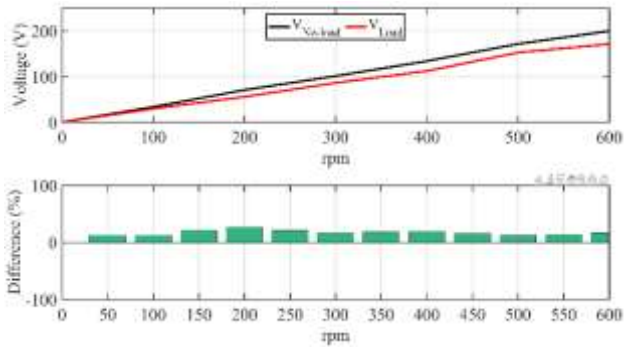

Fig. 12. Evaluation of voltage at different RPM

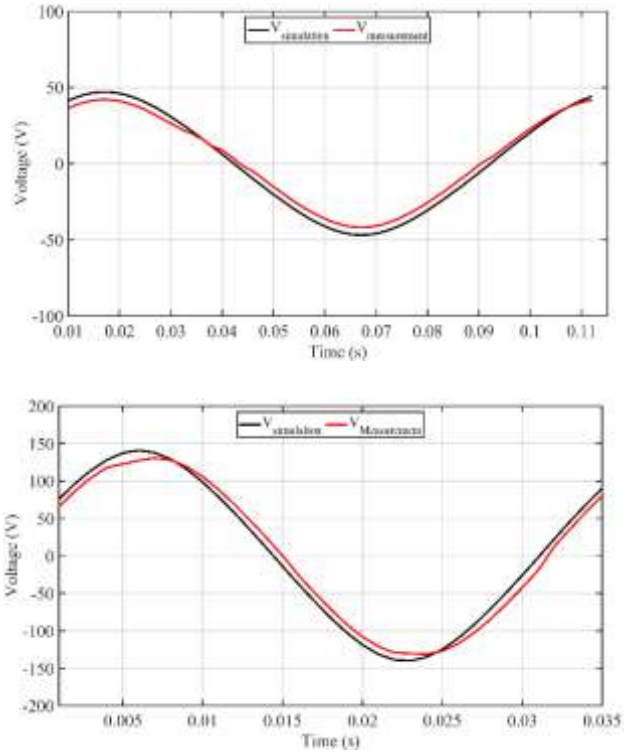

Fig. 13. Voltage signals measured in experimental tests: a) 135 rpm, and b) 385 rpm.

3.4 Total harmonic distortion

The harmonic distortion was evaluated across different operating ranges, as shown in Figure 12. At nominal speed, the total harmonic distortion (THD) is 4.43%, indicating that the generator functions appropriately under these conditions. This value is within the limits set by the IEEE STD 519-2014 [12], which stipulates that for voltages between 1 kV and 69 kV, THD must remain below 5%. Additionally, individual harmonics must not exceed 8%, thus ensuring energy quality and electromagnetic compatibility in electrical systems.

The figure illustrates the behaviour of various harmonic components (3rd, 5th, 7th, 9th, 11th, and 13th) at different RPMs. It is observed that THD remains below 5% throughout the entire operating range, with values increasing significantly at higher speeds, particularly at 535 RPM, where it reaches a maximum of 4.5%. This indicates a slight increase in distortion as the generator operates at higher speeds, but it remains within safe limits.

Additionally, the 3rd harmonic is the most dominant at the measured speeds, especially at 135 RPM and 385 RPM, which peaks at 4.5%. Despite this, it remains below the 8% limit, ensuring the generator complies with safety and performance standards. The 13th harmonic is the least significant of all, with negligible values at all RPMs. Its peak at 535 RPM is still shallow, contributing minimally to the overall harmonic content.

Harmonic distortion analysis across the operating range stays within permissible limits, ensuring the generator operates efficiently and safely. This guarantees minimal interference with other equipment connected to the same electrical system and maintains high energy quality.

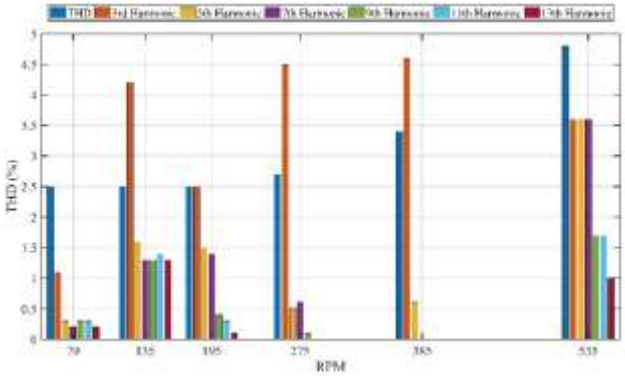

Fig. 12. Evaluation of THD over the wide operating range

3.5 Torque

The PMSG electromagnetic torque is evaluated throughout its entire operating range. Fig. 13 indicates the parametric results for the nominal speed and when the generator operates under load and no-load conditions. Additionally, Fig. 14 presents the electromagnetic torque when the PMSG operates at different speeds. It indicates that the cogging torques are within the permissible range, varying between -0.3 and -1.08 Nm at nominal speed, while the torque ripple at nominal speed is −37.4 Nm, representing 4.4%.

For small-scale generators (up to 100 kW), the permissible cogging torque can range from 0.5 to 5 Nm, and the allowable ripple torque can be less than 1-5% of the nominal torque [13].

Figure 14 includes the results of the cogging torque and torque ripple study for the generator's operating range. It is essential to minimise torque values, as high values can cause noise and vibration, which may lead to rotor deformation. Therefore, torque values should be as low as possible to ensure smooth and efficient machine operation.

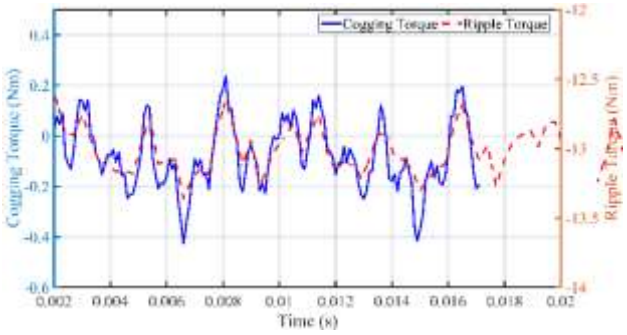

Fig. 13. Cogging and ripple torque at nominal speed

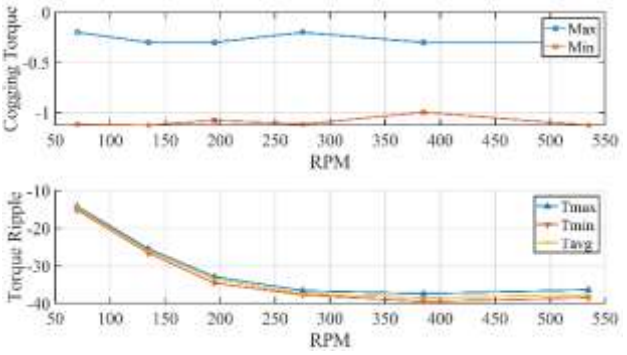

Fig. 14. Evaluation of torque at different RPM

3.6 Losses and power

Figure 15 illustrates the generator's performance under nominal operating conditions. The blue curve represents the power over time, showing a rapid initial increase until it stabilises around 759 W in approximately 0.01 seconds. This indicates that the generator quickly reaches its stable operating regime, a positive sign of its efficiency and responsiveness.

The bar chart in the figure corresponds to power measurements: input power (Pin), output power (Pout), copper losses (Pcu), miscellaneous losses (Pmis), and total power (Ptot), respectively. The copper losses and miscellaneous losses are relatively low compared to the input and output powers, contributing to the system's efficiency.

The generator shows an efficiency of 87% under nominal conditions. This high efficiency suggests a practical design that minimises losses and maximises the valuable power delivered. The rapid power stabilisation and minimal fluctuations after startup reinforce the generator's stability and reliable performance.

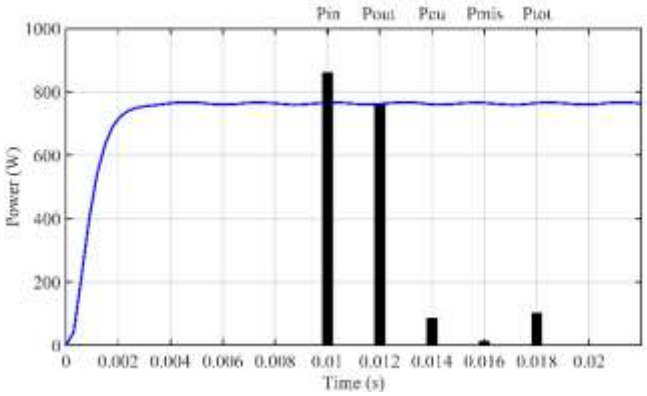

Fig. 15. Generator's performance under nominal operating conditions

3.7 Power Systems Applications

This generator can be used in decentralised installations in modern electrical power systems, providing a reliable and efficient solution for small-scale energy generation. Additionally, future research could focus on improving the reduction of hysteresis losses and further optimising the magnetic flux distribution, allowing for more significant harmonic reduction and, consequently, better overall generator performance.

The integration into distributed generation systems supports the transition toward a more decentralised energy model, enhancing the resilience of the electrical grid and reducing reliance on large power plants. Additionally, part of the research is also focused on improving the aerodynamic design of the rotor to achieve a more efficient and durable system.

Another critical aspect of future research is the development of more efficient methods to integrate these generators with energy storage systems, such as batteries, to improve stability in microgrids and off-grid applications.

4 Conclusion

Efficiency and Cost-Effectiveness: The proposed design methodology for the PMSG has demonstrated remarkable effectiveness. The generator reached an impressive efficiency of 87.1% at full load, validating its suitability for practical use in low-power wind turbines and its potential to improve these systems' economic viability significantly.

Comprehensive Validation: Finite element analysis simulations and experimental testing rigorously confirmed the generator design. The close

correlation between the calculated and measured values of resistance, inductance, and voltage, coupled with a THD of 3.33%, guarantees the accuracy and dependability of the proposed design model.

Magnetic Flux and Voltage Performance: The magnetic flux distribution stays within safe operating parameters, with densities fluctuating between 0 and 1.71 T, indicating no risk of saturation or overheating. The generator produced a voltage of 115 V without load and 108 V with load at nominal speed, demonstrating consistent stability and efficiency in its performance.

Electromagnetic Torque and Losses: The electromagnetic torque parameters, including cogging torque and torque ripple, were within acceptable ranges, minimising noise and vibration. Copper and other losses were comparatively low, with power stabilisation occurring rapidly at approximately 759 W, further supporting the generator's efficiency.

Contribution to Renewable Energy: The study highlights the success of the proposed design in advancing wind energy technology. The developed methodology and generator offer a promising solution for more efficient and cost-effective renewable energy systems, demonstrating its applicability for low-power wind turbine applications.

References

[1] W. Strielkowski, L. Civín, E. Tarkhanova, M. Tvaronavičienė, and Y. Petrenko. "Renewable Energy in the Sustainable Development of Electrical Power Sector: A Review" Energies 14, 2021, no. 24: 8240. https://doi.org/10.3390/en14248240

[2] Global Wind Report 2023; "Global Wind Energy Council, Brussels, Belgium," 2023; Available online: https://gwec.net/globalwindreport2023

[3] T. Kara and D. Şahin-Kara, T, "Implications of Climate Change on Wind Energy Potential". Sustainability 2023, 15, 14822. https://doi.org/10.3390/su152014822

[4] Duane C. Hanselman, Brushless Permanent Magnet Motor Design 2nd Edition. Magna Physics Publishing 2006 (ISBN: 188-1855155).

[5] B. J. Chalmers and E. Spooner, "An axial-flux permanent-magnet generator for a gearless wind energy system," in IEEE Transactions on Energy Conversion, vol. 14, no. 2, pp. 251-257, doi: 10.1109/60.766991.

[6] H. Chun-Yu, Y. Shen-Nian, and H. Jonq-Chin, "Design of High Performance Permanent-Magnet Synchronous Wind Generators," Energies 2014, vol. 11, pp. 7105–7124, November 2014.

[7] R. Bufanio, L. Arribas, J. de la Cruz, T. Karlsson, M. Amadío, A. E. Zappa, and D. Marasco, "An update on the electronic connection issues of low power SWTs in AC-coupled systems: A review and case study," Energies, vol. 15, no. 6, pp. 2082, 2022. Available: https://doi.org/10.3390/en15062082

[8] Z. Zhang, X. Zhang, L. Yu, X. Li, and Y. Xia, "3- D magnetic equivalent circuit model for a coreless axial flux permanent- magnet generator with a rotor back iron," *IET Electric Power Applications*, vol. 15, no. 1, pp. 25-34, 2021, doi: 10.1049/elp2.12044.

[9] S. Kahourzade, A. Mahmoudi, H. W. Ping and M. N. Uddin, "A Comprehensive Review of Axial-Flux Permanent-Magnet Machines," in Canadian Journal of Electrical and Computer Engineering, vol. 37, no. 1, pp. 19-33, winter 2014, doi: 10.1109/CJECE.2014.2309322.

[10] N. Radwan-Pragłowska, T. Wegiel, and D.Borkowski, “Modeling of Axial Flux Permanent Magnet Generators". Energies 2020, 13, 5741. https://doi.org/10.3390/en13215741.

[11] M. Drancă, M. Chirca and Ş. Breban, "Comparative Design Analysis of Axial Flux Permanent Magnet Direct-Drive Wind Generators," 2019 11th International Symposium on Advanced Topics in Electrical Engineering (ATEE), Bucharest, Romania, 2019, pp. 1-5, doi: 10.1109/ATEE.2019.8724928.

[12] IEEE Std 519-2014, "IEEE Recommended Practice and Requirements for Harmonic Control in Electric Power Systems," Institute of Electrical and Electronics Engineers, New York, NY, USA.

[13] IEC 61400-21, "Wind turbines - Part 21: Measurement and assessment of power quality characteristics of grid connected wind turbines," International Electrotechnical Commission, Geneva, Switzerland, 2008.